

# Raman spectroscopic study on structure of human immunodeficiency virus (HIV) and hypericin-induced photosensitive damage of HIV

XU Yiming & LU Chuanzong

Laboratory of Visual Information Processing, Institute of Biophysics, Chinese Academy of Sciences, Beijing 100101, China  
Correspondence should be addressed to Xu Yiming (email: xuliang40@yahoo.com.cn or lvt@sun5.ibp.ac.cn)

Received February 17, 2004; revised July 15, 2004

**Abstract** The first Raman spectra of HIV1- HIV2 in human sera and hypericin-induced photosensitive damage of the virus have been obtained. The prominent Raman lines in the spectra are assigned respectively to the carbohydrates of viral glycoprotein, RNA, protein and lipid. The spectra are dominated by Raman scattering of the carbohydrates. The lines of D-Mannose and N-acetylglucosamine in carbohydrates are obvious and there is a  $\beta$ -configuration in the anomeric C1 position in D-Mannose. The viral RNA duplexes bound assumes an A-form geometry. The lines of backbone phosphate group, bases (involving interbase hydrogen bonding) and ribose of the RNA are complete and distinct. The secondary structure of the viral protein maintains  $\alpha$ -helix,  $\beta$ -sheet,  $\beta$ -turn and random coil. Its side chains are rich and vary from tryptophan, phenylalanine and "buried" tyrosine; the stable conformation of the S-S bond of gauche-gauche-gauche; the two forms of C-S bonds of gauche and trans ; to sulfhydryl group and ionized and unionized carboxyl groups. The viral lipid bilayer molecules are probably in the liquid ordered phase or the gel phase. It was observed that the hypericin-induced photosensitive damage of HIV1-HIV2 in human sera changed various components of HIV1-HIV2 in different degrees : The orderly A-form viral RNA would become a disordered viral RNA. There were a breakage of interbase hydrogen bonds and disruption of vertical base-base stacking interactions. In addition, the groups of ribose and four bases were damaged obviously. A decrease in ordered structure ( $\alpha$ -helix and  $\beta$ -sheet) of viral protein is accompanied by an increase in random coil. The Tyr buried in the three-dimensional structure of protein was damaged, but it was still "buried" and the damage of C-S bond of trans form was stronger. The groups of carbohydrates, including D-Mannose and N-acetyl glucosamine, in viral envelope glycoprotein had also been changed. The hydrophilic C-N bond of choline in viral lipid was damaged, which was the possible binding site to hypericin, whereas the viral lipids bilayers were still probably in the liquid ordered phase or the gel phase. So the space structure of HIV1-HIV2 was damaged under the experimental conditions, which might block viral infection and inhibit its growth and breeding. It is apparent that the laser Raman spectra have provided certain direct evidence at the molecular level for photosensitive damage of HIV1-HIV2.

**Keywords:** HIV1-HIV2, structure, hypericin, photosensitive damage, Raman spectroscopy.

**DOI:** 10.1360/04yc0015

Viruses are agents of some of the most destructive diseases afflicting plants and animals<sup>[1]</sup>. Viruses also play a central role in experimental methods of molecular and cellular biology, especially in modern genetic engineering<sup>[1]</sup>. Raman spectroscopy is a powerful tool for studying the structure of the whole virion. A number of researches are limited to the conformation of viruses, involving only nucleic acid (RNA or DNA) and its coat protein<sup>[1]</sup>. Literatures can be found concerning Raman spectroscopic study of single-stranded RNA viruses, such as tobacco mosaic virus (TMV), turnip yellow mosaic virus (TYMV), belladonna mottle virus (BDMV), cowpea chlorotic mottle virus (CCMV) and bacteriophages R17 and MS2<sup>[1,2]</sup>. Raman spectroscopic study can also be found on filamentous DNA bacteriophages (fd, If1, Iki, Pf1, Xf, Pf3) in single-stranded DNA viruses and that of double-stranded DNA viruses bacteriophages P22 and T7<sup>[1,2]</sup>. The filamentous phage subunit conformation was also analyzed quantitatively<sup>[2]</sup>. In 1996, we reported for the first time "Raman spectroscopic study on human immunodeficiency virus (HIV1—HIV2) space structure and microcosmic and photosensitive damage of hypericin to the virus"<sup>[3]</sup>.

The Acquired Immunodeficiency Syndrome (AIDS) was identified more than 20 years ago<sup>[4–6]</sup>. It is HIV1 and HIV2, two variants, that cause the majority of AIDS in human bodies and constitute one of the principal threats to human life. Aiming to understand and eventually find a cure for AIDS, the HIV virus becomes the most intensively studied virus in human history<sup>[7]</sup>. Great progress has been made in obtaining an outlining sketch of how genes and proteins in HIV virion or virus particles operate and in understanding the biochemical specificity of HIV, the factors controlling its replication, the pathology of how it destroys the human immune system and the molecular bases of HIV infection and immunosuppression<sup>[7–13]</sup>.

In general, the relative amounts of each component of retrovirus are estimated to be about 60%—70% proteins, 30%—40% lipids, 1%—2.5% nucleic acids and 2%—4% carbohydrates<sup>[14,15]</sup>. HIV is a retrovirus. The whole structure of HIV1 is the same as that

of HIV2<sup>[6]</sup>. The outer coat of the HIV virion consists of a lipid bilayer assembled partly from lipid molecules taken from membrane of surrounding host human cells. The lipid bilayer is filled with many proteins, including the viral envelope glycoproteins gp120 and gp41<sup>[7]</sup>. An extensive part of the virion surface is predicted to be covered by carbohydrate<sup>[16]</sup>. The gp120 glycoproteins can bind to the membrane glycoprotein CD4 on the surface of T lymphocytes of the host and the gp41 glycoprotein plays a crucial role in controlling the process of how HIV binds to and enters target cells<sup>[7,16,17]</sup>. The N-linked oligosaccharides chain of gp120 may participate in the interaction with CD4<sup>[16]</sup>. However, it is not clear whether the mannose binding protein, which is bound to gp120, and the carbohydrate mannose play any role in mediating the attachment of the virus to oligosaccharides of host tissues<sup>[16,17]</sup>. There are many other important protein molecules in the HIV virion such as a matrix protein (P17), several capsid proteins (P24, P7) and different enzymes<sup>[7,8]</sup>. The genetic material of HIV consists of two strands of RNA of about 9200 nucleotide bases long each of which fits within the viral core<sup>[4]</sup>. The structures of some of the viral proteins and other components and the relationship between the structure and the function are known<sup>[18–26]</sup>. Their secondary structures or three dimensional structure inside the HIV virion are also studied extensively. It is of interest, for example, to find out the configuration of viral carbohydrates, the state of the lipid bilayer, and the secondary structures of the viral RNA and protein molecules.

Raman spectroscopy is capable of answering structural questions at the molecular level and has been used successfully to study viruses with proteins and nucleic acids as their major components<sup>[27,28]</sup>. We report here for the first time the Raman spectra of human immunodeficiency virus HIV1-HIV2 in human sera. These are the first Raman spectra of complex virus with an RNA, protein, carbohydrate and lipid. The abstract of this paper was presented at the XVth International Conference On Raman Spectroscopy<sup>[3]</sup>. It was demonstrated that HIV1 contains the viral RNA duplexes bound with helix structure<sup>[29]</sup>; the viral pro-

tein maintains  $\alpha$ -helix,  $\beta$ -sheet,  $\beta$ -turn and random coil and there were Tyr, Trp and Phe and so on in HIV1<sup>[29]</sup>, which is in agreement with part of the results in our manuscript<sup>[3]</sup>.

Hypericin (HC), a polycyclic quinone derived from plant genus *Hypericum* (saint-John wort), has been used to prevent uninfected T-cells from being infected with the AIDS virus in cells culture<sup>[30,31]</sup>. It has been known that light plays an important role in some biological events<sup>[30–38]</sup>. HC and some of polycyclic quinines irradiated by light could inhibit HIV-1 replication in cultured cell, inactivated reverse transcriptase and protein kinase C activity *in vitro*<sup>[32–34]</sup>, and inhibit viral fusion<sup>[35–37]</sup>. Degar et al. found evidence for photochemical alterations of HIV1 capsid P24 and a block in uncoating of HIV1<sup>[38]</sup>. An animal test showed that HC had low toxicity at therapeutic doses<sup>[32,39]</sup>. Experiments are needed to elucidate the light-induced interactions between HC and the viral RNA, protein, carbohydrate and lipids.

We first studied the hypericin-induced photosensitive damage of HIV1-HV2 in human sera by laser Raman spectroscopy at the molecular level. Structural information on photosensitive damage of four components—viral RNA, protein, carbohydrate and lipids was obtained. So the characteristics of photosensitive damage of the virus can be deeply investigated, and the anti-AIDS mechanism of the drug further probed. However, it is apparent that more understanding of the mechanisms of photoinactivation should be useful for the development of photodynamic therapies for treatment of AIDS<sup>[40–46]</sup>.

## 1 Materials and methods

### 1.1 Materials

HIV: HIV1 and HIV2 in human serum and negative human sera with 0.1% sodium azide in Target cassettes for the detection of HIV1-HIV2 antibodies (patent No. 4797260) were obtained from V-Tech, Inc. (Pomona CA, U.S.A.). Target HIV1-HIV2 is a rapid immunoenzymatic assay that detects and differentiates anti- HIV1 and anti-HIV2 antibodies in specimens of serum, plasma, or whole blood. The HIV1-HIV2 in

human serum is an enriched liquor required as strong positive control in the test.

Hypericin was purchased from Carl Roth Co. Germany. 15  $\mu$ L HIV1-HIV2 in human sera was mixed with 1  $\mu$ L 32  $\mu$ mol/L hypericin in the buffer to final concentration of 2  $\mu$ mol/L hypericin.

### 1.2 Spectroscopic methods

The Raman spectra of all samples were obtained with a Jobin Yvon model JY-T 800 Raman spectrophotometer (Paris, France) fitted with microcomputer. An argon ion laser (Model 164 from Spectra Physics, CA, U.S.A.) was used as excitation. The experimental conditions were as follows: exciting line 514.5 nm and power 500 mW; the widths of the four slits of the triple monochromator 700, 800, 800, 700  $\mu$ m; step 1  $\text{cm}^{-1}$ ; integral time and signal average: 0.1 s and 7 scans (450–1750  $\text{cm}^{-1}$ ), 0.2 s and 5 scans (2500–2600  $\text{cm}^{-1}$ ), 0.2 s and 2 scans (2800–3100  $\text{cm}^{-1}$ ), room temperatures  $18 \pm 2^\circ\text{C}$ . The vibrational frequencies in  $\text{cm}^{-1}$  and tentative assignments are listed in table 1.

## 2 Results and discussions

### 2.1 The space structure of protein, RNA, carbohydrate and lipid bilayer in HIV

Fig. 1 shows the Raman spectra of HIV1-HIV2 in human serum and the negative human serum used as a control in selected regions of interest between 450 and 3100  $\text{cm}^{-1}$ . More details of the Raman spectra in fig. 1 are shown in figs. 2–4 in different spectral regions. It is clear from fig. 1 that the major contribution of the Raman signal from the HIV1-HIV2 sample is from the virus. Their characteristic Raman frequencies in  $\text{cm}^{-1}$  and assignments are listed in table 1.

In contrast, the prominent Raman lines in the Raman spectra of HIV1-HIV2 in human serum have contributions from all four major components of the virus. Peaks can be assigned to the carbohydrates of the viral glycoprotein, proteins including different enzymes, the two strands of the RNA, and lipids, respectively (figs. 1–3)<sup>[28,29,47–60]</sup>. In some cases, a peak has contribution from more than one component.

Table 1 Raman spectra of HIV1 -HIV2 in human serum at 18 °C ( 450–3100 cm<sup>-1</sup>)

| Frequency/cm <sup>-1</sup> | Assignment                            |         |          |         |
|----------------------------|---------------------------------------|---------|----------|---------|
|                            | carbohydrate                          | RNA     | protein  | lipid   |
| 465                        |                                       |         |          |         |
| 493                        | Man                                   |         |          |         |
| *503                       | skeletal modes                        | r       | S-S str  |         |
| 515                        | GlcNac                                |         | S-S str  |         |
| 548                        |                                       |         | Trp      |         |
| 581                        |                                       | C, G    | Trp      |         |
| 596                        |                                       | C       |          |         |
| 602                        | Man                                   |         |          |         |
| 613                        |                                       |         |          |         |
| 620                        |                                       |         | Phe      |         |
| *631                       | GlcNac                                | r       |          |         |
| 640                        |                                       |         | Tyr      |         |
| 669                        | Man                                   | G       |          |         |
| 676                        |                                       |         |          |         |
| 684                        |                                       |         |          |         |
| 692                        |                                       |         |          |         |
| 703                        | GlcNac                                |         | C-S str  |         |
| 717                        |                                       |         | C-S str  | C-N sym |
| 728                        |                                       | A       |          |         |
| 736                        | GlcNac                                |         |          |         |
| * 743                      | Man                                   |         | Ile, Asn |         |
| 751                        |                                       | C       |          |         |
| 759                        |                                       |         | Trp, Val |         |
| 769                        | Man                                   |         |          |         |
| 778                        |                                       |         |          |         |
| 786                        |                                       | C, U    | Thr      |         |
| 814                        |                                       | O—P—O   | Asn      |         |
| * 832                      | Man                                   |         | Tyr, Val |         |
| * 851                      |                                       |         | Tyr      |         |
| 859                        |                                       |         |          |         |
| 880                        | β-C1 config.<br>Man                   |         | Trp, Val |         |
| 907                        | Man                                   |         | C-C str  |         |
| * 926                      | COH bending                           |         | C-C str  |         |
| 933                        | GlcNac                                |         | C-C str  |         |
| 952                        | Man                                   |         | C-C str  |         |
| 974                        | Man                                   | r       |          |         |
| 994                        | CH <sub>2</sub> rock                  |         |          |         |
| *1004                      |                                       | r       | Phe      |         |
| 1048                       | C1-H bending, Man<br>C-O, C-C, GlcNac | r       | C-N str  |         |
| 1089                       | COH bending                           |         | C-N str  | C-C str |
| 1106                       | Man                                   | O=P=O   |          |         |
| * 1123                     | Man, GlcNac                           | C, U    | C-N str  | C-C str |
| 1132                       | Man                                   |         | C-N str  |         |
| 1157                       |                                       | r       | C-N str  |         |
| 1172                       |                                       |         |          |         |
| 1178                       |                                       | G, A, C | Tyr      |         |
| 1193                       |                                       |         |          |         |
| *1205                      |                                       |         | Tyr, Phe |         |

(To be continued on the next page)

(Continued)

| Frequency/cm <sup>-1</sup> | Assignment                                  |                         |                          |                         |
|----------------------------|---|-------------------------|--------------------------|-------------------------|
|                            | carbohydrate                                | RNA                     | protein                  | lipid                   |
| *1226                      |   | A                       | Amide III                |                         |
| 1237                       |   | U, C                    | Amide III                |                         |
| 1244                       |   |                         | Amide III                |                         |
| *1250                      |   | A, C                    | Amide III                |                         |
| 1264                       |   |                         | Amide III                |                         |
| 1277                       | COH, Man                                    |                         | Amide III                |                         |
| 1282                       |   |                         |                          |                         |
| 1303                       |   | A, C                    | Amide III                |                         |
| 1322                       | GlcNac                                      | G                       | C-H def                  |                         |
| 1330                       | C(6)-H <sub>2</sub> , CH <sub>3</sub> , COH |                         |                          |                         |
| *1341                      |   | A                       | C-H def, Trp             |                         |
| 1348                       | COH, Man                                    |                         |                          |                         |
| 1356                       |   |                         | Trp                      |                         |
| 1379                       | CH <sub>3</sub> , GlcNac, Man               | G, U, A                 |                          |                         |
| 1394                       |   |                         |                          |                         |
| 1408                       | Man   |                         | CO <sub>2</sub> -sym str |                         |
| 1419                       |   | G, A                    |                          |                         |
| 1433                       | GlcNac                                      |                         | Trp(N-H def)             |                         |
| *1456                      | CH <sub>2</sub> bending                     | CH <sub>2</sub> bending | CH <sub>2</sub> bending  |                         |
| 1484                       |   | G, A                    |                          |                         |
| 1494                       |   |                         |                          |                         |
| 1508                       |   | A                       |                          |                         |
| 1520                       |   |                         |                          |                         |
| 1527                       |   | C                       |                          |                         |
| 1537                       |   | G                       |                          |                         |
| 1555                       | GlcNac(Amid II)                             |                         | Amide II, Trp            |                         |
| 1567                       |   |                         |                          |                         |
| 1581                       |   | G, A                    | Trp                      |                         |
| 1613                       |   |                         |                          |                         |
| 1620                       | Man   | C=O str, U              | Trp, Tyr, Phe            |                         |
| 1628                       |   |                         |                          |                         |
| 1635                       | GlcNac(Amide I)                             |                         |                          |                         |
| 1644                       |   |                         | Amide I                  |                         |
| 1660                       |   | C=O str,<br>U, G, C     | Amide I                  |                         |
| 1669                       |   |                         | Amide I                  |                         |
| 1696                       |   |                         |                          |                         |
| 1725                       |   |                         | C=O str                  |                         |
| *2552                      |   |                         | S-H str, Cys             |                         |
| 2578                       |   |                         | S-H str, Cys             |                         |
| 2853                       |   |                         |                          | CH <sub>2</sub> sym str |
| 2883                       |   |                         | C-H str                  | CH <sub>2</sub> asystr  |
| 2900                       | C-H str                                     |                         |                          |                         |
| *2935                      | C-H str                                     | C-H str                 | C-H str                  | C-H str                 |
| *2979                      | C-H str                                     | C-H str                 | C-H str                  |                         |

\*The common vibration mode of both HIV1-HIV2 and negative human serum is noted. +Abbreviations: Man, D-Mannose; GlcNac, N-acetylglucosamine; Tyr, tyrosine; Trp, tryptophan; Phe, phenylalanine; O-P-O, PO<sub>2</sub>; O=P=O, PO<sub>2</sub>; r, ribose; A, adenine; G, guanine; C, cytosine; U, uracil; sym, symmetric; asym, asymmetric; str, stretching; def, deformation.

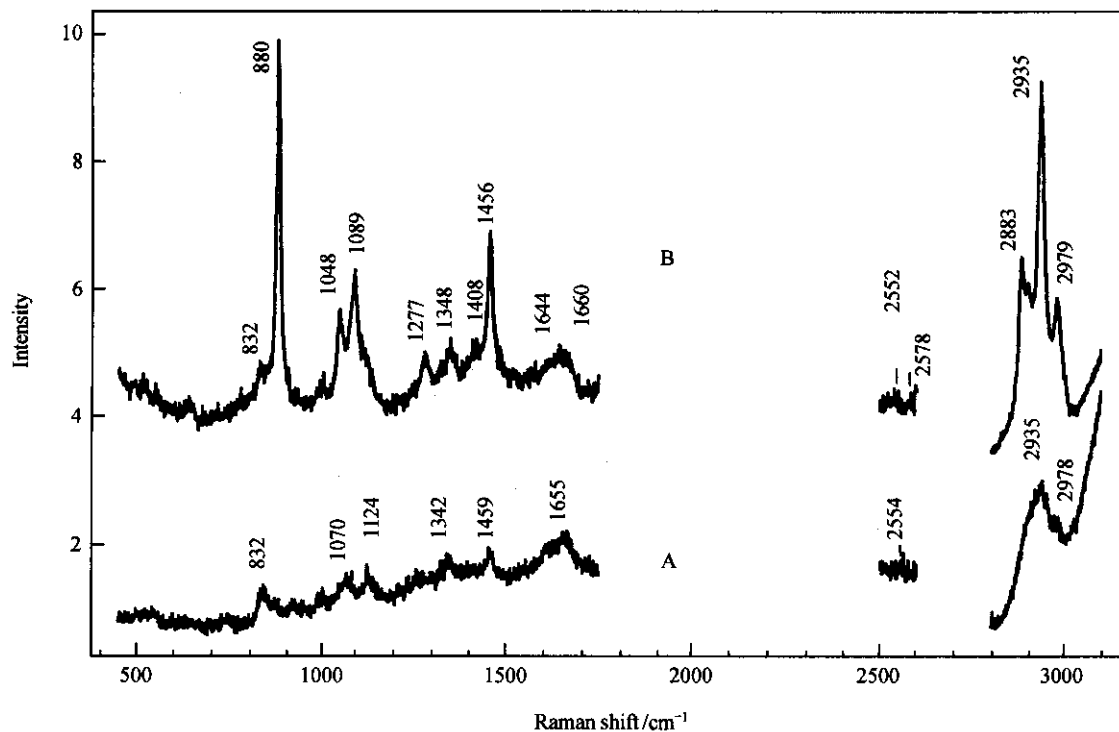


Fig. 1. Raman spectra of negative human serum (A) and HIV1-HIV2 in human serum ( $450\text{--}3100\text{ cm}^{-1}$ ) (B).

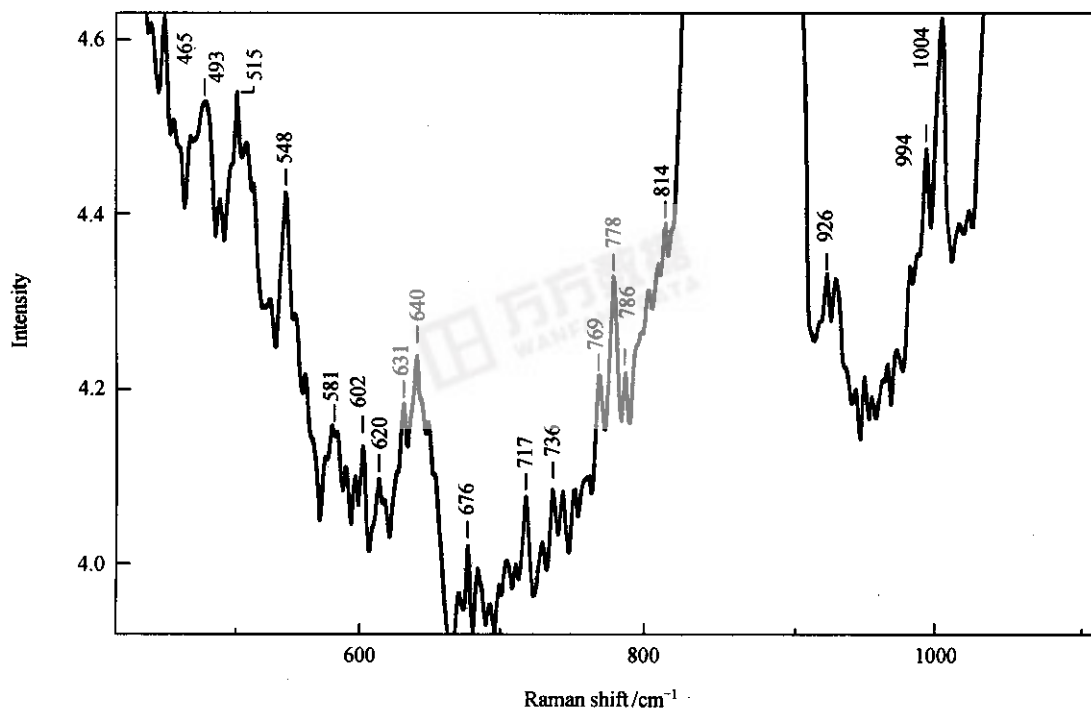


Fig. 2. Raman spectra of HIV1-HIV2 in human serum ( $450\text{--}1100\text{ cm}^{-1}$ ).

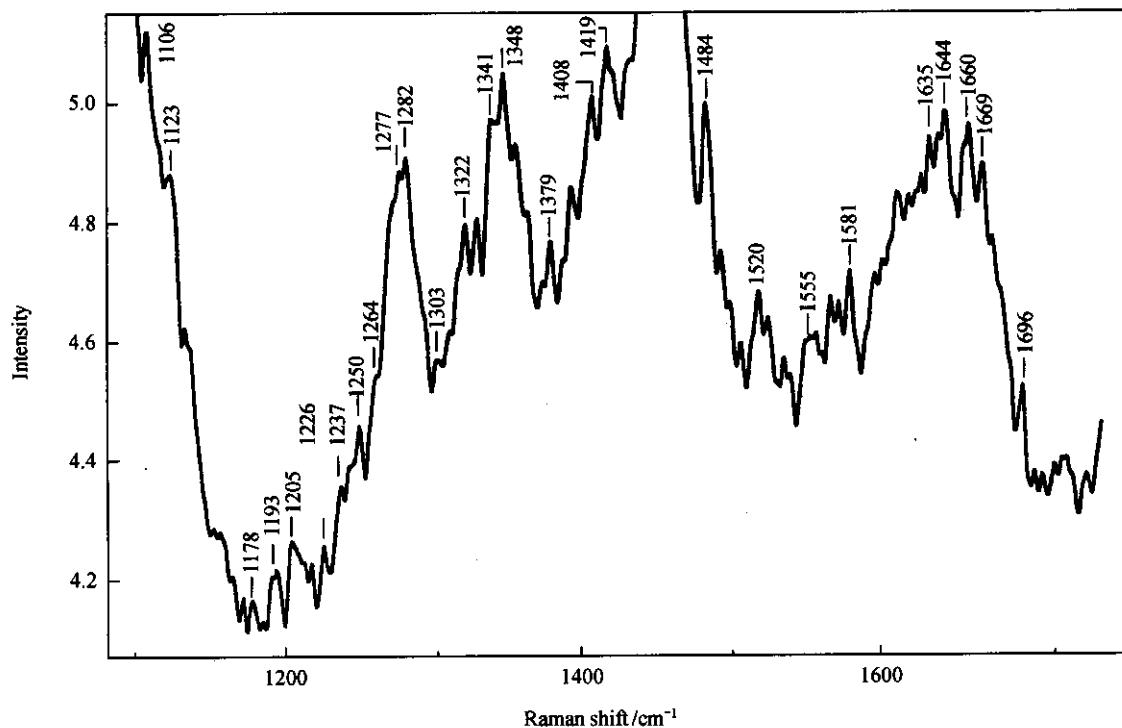


Fig. 3. Raman spectra of HIV1-HIV2 in human serum (1100–1750  $\text{cm}^{-1}$ ).

(i) Raman spectra of the carbohydrates of HIV1-HIV2 in human sera. 50% of the molecular mass of the major envelope glycoprotein is carbohydrate in the form of an array of oligosaccharide structures attached to the polypeptide backbone<sup>[16]</sup>. An extensive part of the virion surface is predicted to be covered by carbohydrates<sup>[16]</sup>. In addition, their Raman activities are stronger, so the lines intensities of carbohydrates are very high. Raman spectra of HIV1-HIV2 in human serum are dominated by Raman scattering of the constituent carbohydrates. The strong lines occurring at 880, 1048, 1089, 1277, 1348, 1456  $\text{cm}^{-1}$  and 2935, 2979  $\text{cm}^{-1}$  belonged to carbohydrates molecules in HIV1-HIV2<sup>[50–52,56]</sup>. The band at 1048  $\text{cm}^{-1}$  is assigned to C1–H bending vibration. The vibrational mode may be associated with either the CCH group or the OCH group, or a combination of the two<sup>[50,51]</sup>. There was the line assigned to COH bending at 1089  $\text{cm}^{-1}$ <sup>[50,51]</sup>. The lines belonging to the vibrational mode of the COH, COH and CH<sub>2</sub> bending appeared at 1277, 1348 and 1456  $\text{cm}^{-1}$ , respectively<sup>[50,51]</sup>. The lines assigned to C-H stretching vibration at 2935 and

2979  $\text{cm}^{-1}$ <sup>[51]</sup>. And two lines at 503 and 515  $\text{cm}^{-1}$  probably belonged to the skeleton of the carbohydrate<sup>[52]</sup>. Mannose and N-acetylglucosamine were the main component of gp120's oligosaccharide<sup>[16]</sup>. The strong lines occurring at 880, 1048, 1277 and 1348  $\text{cm}^{-1}$  clearly also were assigned to D-Mannose<sup>[52]</sup>. The strong line at 880  $\text{cm}^{-1}$  belonged to the  $\beta$ -configuration in the anomeric C1 position of D-Mannose<sup>[52]</sup>. The strong line belonging to N-acetyl glucosamine appeared at 1048  $\text{cm}^{-1}$ , and middle or weak lines that occurred at 631, 736, 1322, 1330 (C(6)–H<sub>2</sub>, CH<sub>3</sub>, COH), 1379 (CH<sub>3</sub>), 1555 (Amid II) and 1635  $\text{cm}^{-1}$  (Amide I), respectively<sup>[56]</sup>.

(ii) Raman spectra of the protein of HIV1-HIV2 in human serum. There are encoding 15 distinct proteins<sup>[29]</sup> including a matrix protein (P17) that forms a layer underneath the envelope, a capsid protein (P24) that makes up the core, protein P6, nucleocapsid protein P7 and several important enzymes including a protease, a reverse transcriptase and an integrase<sup>[7,8,29]</sup>, in addition, the protein in the two major glycoproteins

gp41 and gp120<sup>[7,29]</sup>.

**Main chain conformation:** The amide I and amide III modes of the backbone are known to be sensitive to the secondary structure of proteins<sup>[47–49,53,54]</sup>. In the amide III region, the peak at ca. 1226 and 1237  $\text{cm}^{-1}$  can be assigned to  $\beta$ -sheet and those at ca. 1264 and 1277  $\text{cm}^{-1}$  to  $\alpha$ -helix<sup>[47–49]</sup>. Similarly the peak at ca. 1303  $\text{cm}^{-1}$  is due to  $\beta$ -turn<sup>[53–54]</sup> and those at ca. 1244 and 1250  $\text{cm}^{-1}$  to random coil<sup>[47,49]</sup>. The main chain conformation of HIV1's protein was also researched through the crystal structure analysis of protein and NMR technique. It was indicated that  $\alpha$ -helix,  $\beta$ -sheet,  $\beta$ -turn and random coil also existed in HIV1<sup>[29]</sup>.

C–C and C–N backbone stretching vibrations are also sensitive to protein conformation. For example, the C–C stretching modes at 907, 926, 933 and 952  $\text{cm}^{-1}$  suggest the presence of  $\alpha$ -helix and random coil, respectively<sup>[47–50]</sup>. The lines assigned to C–N stretching vibrations occur at 1048, 1089, 1123, 1132 and 1157  $\text{cm}^{-1}$ <sup>[47]</sup>. Some of the strongest lines are due to the main chain also. The  $\text{CH}_2$  bending mode at ca. 1456  $\text{cm}^{-1}$  and C–H stretching vibrations at 2935 and 2979  $\text{cm}^{-1}$  are very clear and strong<sup>[47]</sup>. Finally, the lines at 1322 and 1341  $\text{cm}^{-1}$  can be assigned to C–H deformation with major contribution expected from the main chain<sup>[47–49]</sup>.

**Side chain conformation:** Most of the peaks due to side chain of the protein are from the aromatic residues<sup>[47–49]</sup>. For example, the indole ring mode of tryptophan can be found in the Raman spectra of HIV1-HIV2 at ca. 548, 581, 759, 880, 1341, 1356, 1433, 1555, 1581 and 1620  $\text{cm}^{-1}$ , the p-hydroxy phenyl ring mode of tyrosine at ca. 640, 832, 851, 1178, 1205 and 1620  $\text{cm}^{-1}$ , and the mono-substituted phenyl ring modes of phenylalanine at ca. 620, 1004, 1205 and 1620  $\text{cm}^{-1}$ <sup>[47–49]</sup>. The double peaks of tyrosine at 832 and 851  $\text{cm}^{-1}$  come from the Fermi resonance between a ring breathing vibration and an overtone of an out-of-plane ring bending vibration<sup>[48]</sup>. The intensity ratio (I<sub>850</sub>/I<sub>830</sub>) is sensitive to the nature of hydrogen bonding and/or the state of ionization of the phenolic hydroxyl group<sup>[48]</sup>. The ratio of two peaks in our spec-

tra is 0.91, suggesting that these tyrosine residues are “buried”<sup>[48]</sup>.

The disulfide bond and sulfhydryl group can also be observed. The cysteinyl S–H stretching mode can be found at 2552 and 2578  $\text{cm}^{-1}$ <sup>[47–49]</sup>. The peaks from the S–S bond stretching vibrations are at 503 and 515  $\text{cm}^{-1}$ , indicating that the conformation of the C–S–S–C is the gauche-gauche-gauche<sup>[47–49]</sup>. Furthermore, the peaks at 631, 640  $\text{cm}^{-1}$  and 703, 717  $\text{cm}^{-1}$  can be assigned to the two conformations of gauche and transforms of C–S stretching vibration, respectively<sup>[47–49]</sup>.

Modes from the carboxyl group of the aspartic acid and glutamic acid residues can also be observed. The peak at ca. 1725  $\text{cm}^{-1}$  is likely to be due to the unionized –COOH group<sup>[47]</sup> while the peak at ca. 1408  $\text{cm}^{-1}$  is from the ionized –COO<sup>–</sup> group<sup>[47]</sup>. The information of side chain conformation of viral protein has not been reported till now.

(iii) Raman spectra of the RNA of HIV1-HIV2 in human serum. Frankal et al. reported HIV1 contains two identical RNA with a six-base pair helix that forms “hairpins” structure<sup>[29]</sup> in 1998. We demonstrated that the viral double helical RNA exists in HIV1–HIV2 in human serum by Raman spectroscopy in 1996<sup>[3]</sup>.

**Space structure of backbone phosphate group and ribose:** The line assigned to backbone phosphate diester (PO<sub>2</sub>) symmetric stretching at 814  $\text{cm}^{-1}$  is clear. It is indicated that the viral RNA duplexes bound assumes an A-form geometry<sup>[3,28]</sup>. The line assigned to backbone phosphate ion (PO<sub>2</sub><sup>–</sup>) symmetric stretching occurred at 1106  $\text{cm}^{-1}$ <sup>[27,28]</sup>. The average conformation of backbone phosphate ion in the virus is apparently different from that of protein-free RNA. The characteristic frequency is 1106  $\text{cm}^{-1}$  in the former, whereas the characteristic frequency is 1100  $\text{cm}^{-1}$  in the latter<sup>[28]</sup>. The lines belonging to C–O and C–C stretching vibration of ribose in the viral RNA appeared at 974, 1048 and 1157  $\text{cm}^{-1}$ , respectively<sup>[27,28]</sup>.

**Conformation of bases:** The lines assigned to ring stretching vibration of bases in the viral RNA occurred

at 669(G), 728(A), 751(C), 786(C, U), 1123(C, U), 1178(G, A, C), 1226(A), 1237(U, C) 1250(A, C), 1484(G, A), 1508(A), 1527(C) and 1537(G)  $\text{cm}^{-1}$ , respectively<sup>[28,55]</sup>. The lines assigned to ring stretching and CH deformation vibrations occurred at 1303(A, C), 1322(G), 1341(A), 1379(G, U, A), 1419(G, A)  $\text{cm}^{-1}$ , respectively<sup>[28,55]</sup>. The line at 1581(G,A)  $\text{cm}^{-1}$  is assigned to C=N and C=C stretching vibrations<sup>[28,55]</sup>. The lines appearing at 1620(U) and 1660(U, G, C)  $\text{cm}^{-1}$  belonged to C=O stretching vibrations<sup>[28,55]</sup>, involved in interbase hydrogen bonding<sup>[28]</sup>.

(iv) Raman spectra of the lipids of HIV1-HIV2 in human serum. The lines assigned to lipids of the viral membrane appeared at 717, 1089, 1123, 1456, 2853, 2883 and 2935  $\text{cm}^{-1}$ , respectively<sup>[56–60]</sup>. They are assigned to C–N symmetrical stretching of choline group, C–C skeletal (gauche and trans), CH<sub>2</sub> bending and C–H stretching vibrations<sup>[56–60]</sup>, respectively. Comparing Raman spectra of HIV1-HIV2 in human serum with negative human serum at 2800–3100  $\text{cm}^{-1}$ , it was found that the former was of these bands appearing at 2853 and 2883  $\text{cm}^{-1}$  while the latter not. The intensity ratio ( $I_{\text{CH}}$ )  $I_{2883}/I_{2853}$  of the two bands assigned to asymmetrical and symmetrical C–H stretching vibration of methylene (–CH<sub>2</sub>–) at 2883 and 2853  $\text{cm}^{-1}$ , respectively, is quite sensitive to the changes of conformation of lipid. The order parameter for the lateral packing of lipids  $S_{\text{lat}}$  which reflected the state of lateral packing of the lipid bilayer was used widely to study the structure of membranes<sup>[56–60]</sup>. The band at 2883  $\text{cm}^{-1}$  is involved in C–H stretching vibration of the viral protein<sup>[28]</sup>. The intensity ratio is about 5.6, so  $S_{\text{lat}}$  was 3.3, therefore the lipid bilayer molecules in HIV1-HIV2 are probably in liquid ordered phase or gel phase<sup>[56–60]</sup>. The fine and close outer coat-envelope consisting of lipid bilayers would effectively protect various viral proteins, enzymes and RNA genomes.

To sum up, the prominent lines in Raman spectra of HIV1-HIV2 in human serum are respectively assigned to carbohydrates of the viral glycoprotein, RNA, protein and lipid. The spectra are dominated by Raman scattering of the carbohydrates. The lines of D-

Mannose and N-cetylglucosamine in carbohydrates are obvious and there is  $\beta$ -configuration in the anomeric C1 position in D-Mannose. The viral RNA duplexes bound assumes an A-form geometry. The lines of backbone phosphate group, bases (involving interbase hydrogen bonding) and ribose of the RNA are complete and distinct. The secondary structure of the viral protein maintains  $\alpha$ -helix,  $\beta$ -sheet,  $\beta$ -turn and random coil. Its side chains are rich and vary from tryptophan, phenylalanine and “buried” tyrosine; the stable conformation of the S–S bond of gauche-gauche-gauche; the two forms of C–S bonds of gauche and trans; to sulfhydryl group and ionized and unionized carboxyl groups. The viral lipid bilayer molecules are probably in the liquid ordered phase or the gel phase.

(v) Raman spectra of the negative human serum. The strong lines in the Raman spectrum of the negative human serum can be assigned to be due to protein (see fig. 4). For example, the backbone modes of amide I and III can be found in the region around 1660  $\text{cm}^{-1}$  and 1220 to 1300  $\text{cm}^{-1}$  respectively. The peaks at ca. 1655  $\text{cm}^{-1}$  are typical amide I peak of  $\alpha$ -helix<sup>[47–49]</sup>. Similarly, in the amide III region, the 1226 and 1232  $\text{cm}^{-1}$  peaks can be assigned to  $\beta$ -sheet, the 1253  $\text{cm}^{-1}$  peak to random coil and 1299  $\text{cm}^{-1}$  to  $\alpha$ -helix<sup>[47–49]</sup>, respectively. It is interesting to note that there seems to be no  $\beta$ -turn<sup>[47–49]</sup>. The other strong peaks can also be assigned to protein such as the peaks at ca. 500, 521, and 543  $\text{cm}^{-1}$  to S-S stretch, 832 and 852  $\text{cm}^{-1}$  to tyrosine, 1003  $\text{cm}^{-1}$  to phenylalanine, a weak peak at 2554  $\text{cm}^{-1}$  to S–H stretch<sup>[26–28]</sup>, 1070  $\text{cm}^{-1}$  to C–N stretch, 1342  $\text{cm}^{-1}$  to C–H deformation, 1459  $\text{cm}^{-1}$  to CH<sub>2</sub> bending, and 2935 and 2978  $\text{cm}^{-1}$  to C–H stretch, respectively<sup>[47–49]</sup>. The proteins in the negative human serum do not contain tryptophan. In addition, there is no contribution from lipid, carbohydrate and RNA in the Raman spectra of the negative human serum.

## 2.2 Hypericin-induced photosensitive damage of HIV

The structure of hypericin is shown in Scheme 1.

The Raman spectra of HIV1-HIV2 in human serum before and after being exposed to light in the

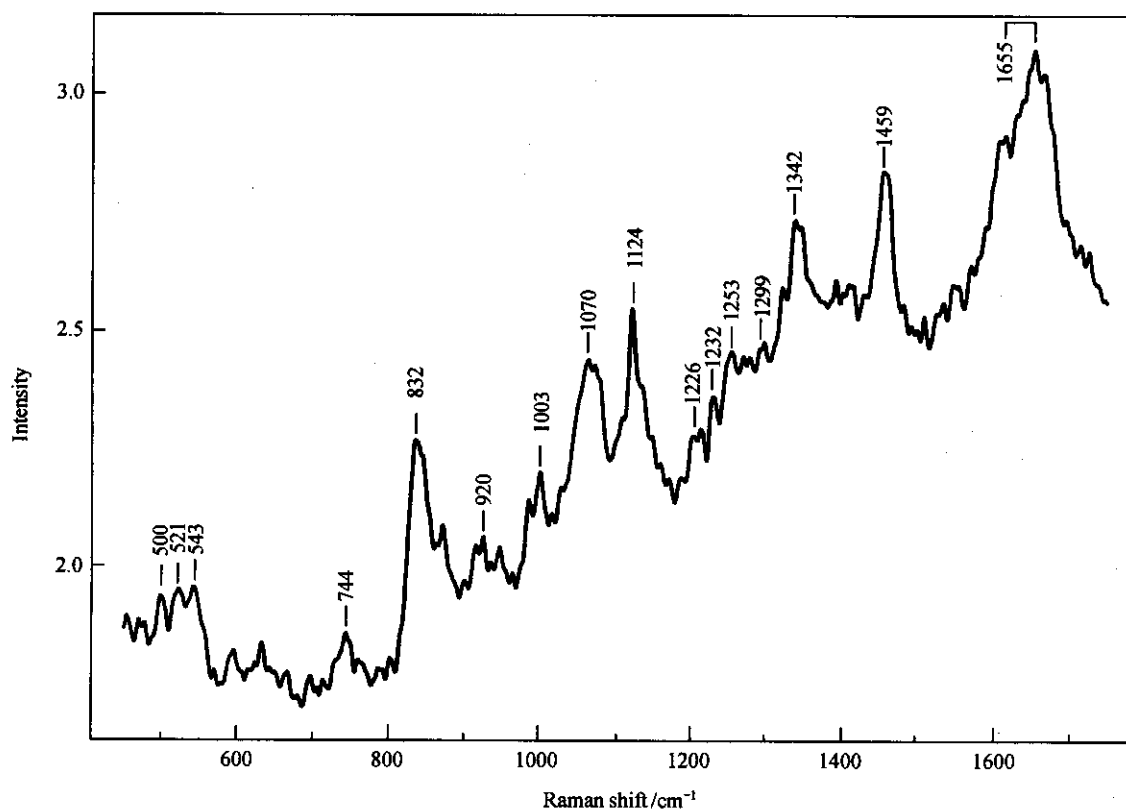
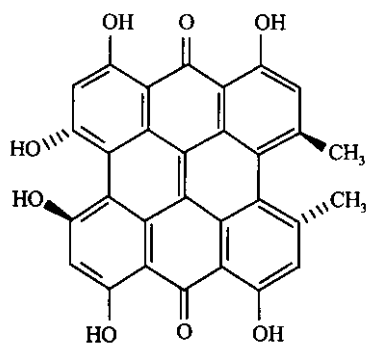


Fig. 4. Raman spectra of the negative human serum (450—1750  $\text{cm}^{-1}$ ).



Scheme 1. Structure of hypericin.

presence of hypericin (HC) are shown in fig. 5. More details of the Raman spectra in fig. 5(b) are shown in figs. 6 and 7 in different spectral regions. It is obvious that the major contribution of the Raman signal is from the HIV1-HIV2. There was no signal of HC observed. We have compared Raman spectra of HIV1-HIV2 in human serum before and after the photosensi-

tive damage. The intensity and position of the line assigned to the breathing vibration of the monosubstituted phenyl ring of phenylalanine at  $1004 \text{ cm}^{-1}$ , which is insensitive to conformational change<sup>[47,48]</sup>, was not changed by the photosensitive damage under the experimental conditions. Therefore this special line was used as the inner standard to determine the relative intensity of other lines of HIV1-HIV2 in human serum. The intensity of Raman line is proportional to the number of scattering centers<sup>[61,62]</sup>. Therefore, when line intensity decreased, it meant the decrease of the number of scattering centers, such as the groups and chemical bonds. Change rates in line intensities of various groups of HIV1-HIV2 were correlated to the damaged degree. The shoulder peak was not determined. The common lines of some groups were also recorded to investigate the structure changes of HIV1-HIV2 damaged.

(i) The photosensitive damage of the viral car-

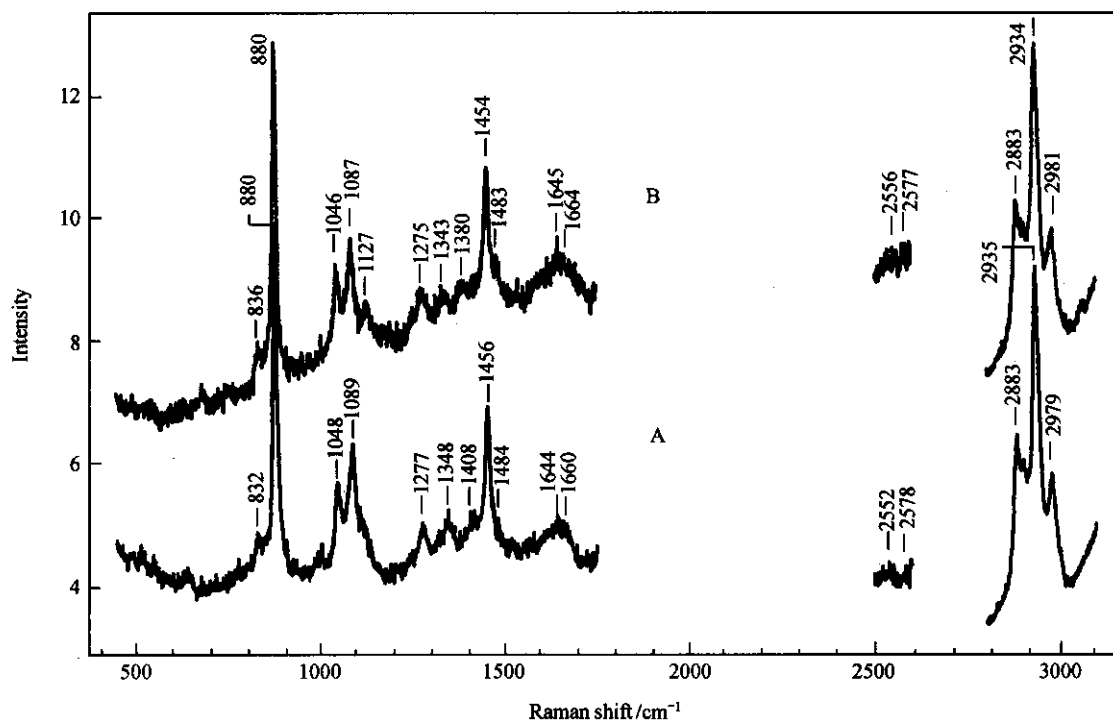


Fig. 5. Raman spectra of HIV1-HIV2 in human serum before (A) and after (B) hypericin-induced photosensitive damage ( $450\text{--}3100\text{ cm}^{-1}$ ).

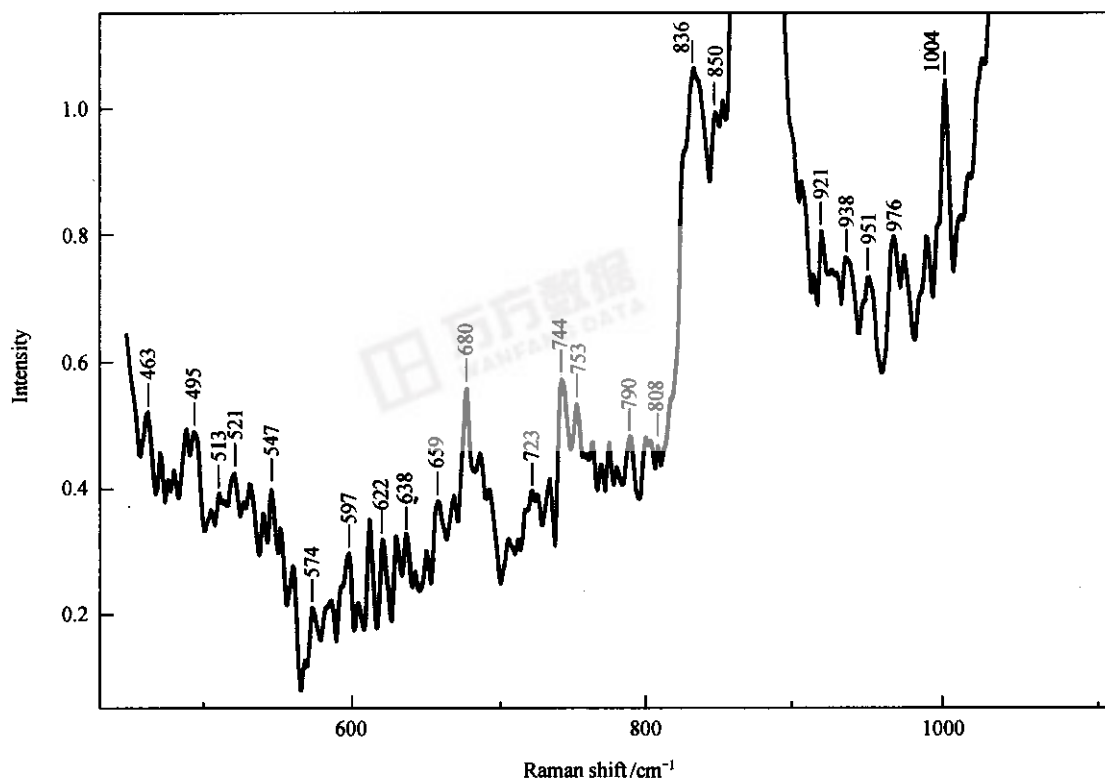


Fig. 6. Raman spectra of HIV1-HIV2 in human serum after hypericin-induced photosensitive damage ( $450\text{--}1100\text{ cm}^{-1}$ ).

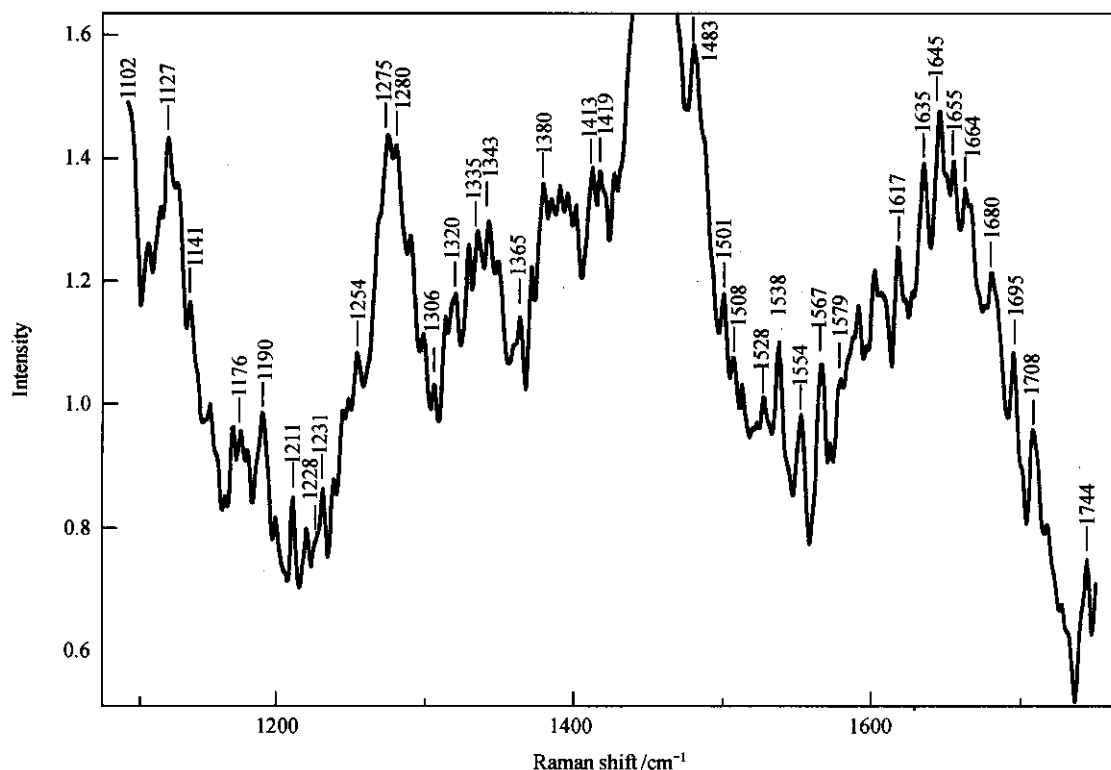


Fig. 7. Raman spectra of HIV1-HIV2 in human serum after hypericin-induced photosensitive damage (1100–1750  $\text{cm}^{-1}$ ).

bohydrates. It is important to understand HC-induced photosensitive damage of the carbohydrates, since 50% of the molecular mass of the major envelope glycoprotein is carbohydrate<sup>[20]</sup>. The intensities of the strong lines at 880, 1048, 1089, 1277, and 1456  $\text{cm}^{-1}$ , respectively, assigned to  $\beta$ -configuration in the anomeric C1 position of D-Mannos<sup>[50–52]</sup>, C1–H bending vibration, the vibrational mode may be associated with either the CCH group or the OCH group, or a combination of the two. COH bending, COH and  $\text{CH}_2$  bending<sup>[50–52]</sup> somewhat decreased, whereas strong lines belonging to COH<sup>[52]</sup> at 1348  $\text{cm}^{-1}$  shifted to 1343  $\text{cm}^{-1}$  and its line intensities decreased by 41%. The line at 513  $\text{cm}^{-1}$  is probably due to the skeleton of the carbohydrates<sup>[50,51]</sup> and decreased by 72%. It suggested that damage of the skeletons of the viral carbohydrates was stronger. S–S bond of the protein also contributed to the line at 513  $\text{cm}^{-1}$ <sup>[47]</sup>. The line intensities assigned to GlcNac,  $\text{CH}_2$  rock and GlcNac(C(6)- $\text{H}_2$ ,  $\text{CH}_3$ , COH) at 631, 994 and 1330  $\text{cm}^{-1}$ <sup>[51,56,63]</sup> decreased by 52%, 38% and 9%, respectively. The

ribose of RNA also contributed to the line at 631  $\text{cm}^{-1}$ . It is evident that the photosensitive damage of viral carbohydrates would affect the interaction of  $\text{CD}_4$  with gp120 that plays important roles in viral infectivity<sup>[16,8]</sup>.

(ii) The photosensitive damage of the viral protein

Main chain conformation: The lines assigned to the main chain amide I and amide III of the viral protein are sensitive to the change in protein conformation<sup>[47–49]</sup>. The line assigned to  $\alpha$ -helix<sup>[47–49]</sup> at 1264  $\text{cm}^{-1}$  disappeared. The peak belonging to  $\beta$ -sheet at 1226  $\text{cm}^{-1}$  changed into shoulder peak which shifted to 1228  $\text{cm}^{-1}$  and the line assigned to  $\beta$ -turn at 1303  $\text{cm}^{-1}$  (Amide III)<sup>[53,54]</sup> shifted to 1306  $\text{cm}^{-1}$ . The line assigned to  $\alpha$ -helix or random coil at 1660  $\text{cm}^{-1}$ <sup>[47–49]</sup> shifted to 1664  $\text{cm}^{-1}$ , which was assigned to random coil<sup>[47–49]</sup>. The line at 1669  $\text{cm}^{-1}$  assigned to  $\beta$ -sheet or random coil<sup>[47,49]</sup> disappeared. It was noted that a decrease in orderly structure ( $\alpha$ -helix and  $\beta$ -sheet) was

followed by an increase in random coil in the viral proteins.

C—C and C—N backbone stretching vibrations are also sensitive to the changes in protein conformation<sup>[47–49]</sup>. The lines of  $\alpha$ -helix of C—C stretching vibration shifted from 907, 926 and 933  $\text{cm}^{-1}$  to 908, 928 and 938  $\text{cm}^{-1}$ <sup>[47–49]</sup>. The line intensity at 951  $\text{cm}^{-1}$ , which was assigned to random coil of C—C stretching vibration, increased by 123%. The lines of C—N stretching vibrations at 1046, 1123, 1132 and 1157  $\text{cm}^{-1}$  shifted to 1048, 1127, 1141 and 1155  $\text{cm}^{-1}$ <sup>[47–49]</sup>, respectively. Their lines intensities also changed in different degree.

Side chain conformation: The lines of S—S bond stretching vibration at 503 and 515  $\text{cm}^{-1}$  shifted to 506 and 513  $\text{cm}^{-1}$ , respectively. The line intensities at 513  $\text{cm}^{-1}$ , which were assigned to gauche-gauche-gauche<sup>[47–49]</sup>, decreased by 72%. The skeleton of the carbohydrates also contributed to the line at 513  $\text{cm}^{-1}$ , in addition conformation of S—S bond had no change, so its damage might be weaker whereas damage of the skeleton of the carbohydrates might be stronger. The lines at 703 and 717  $\text{cm}^{-1}$ , which belonged to trans form of C—S stretching vibration<sup>[47–49]</sup>, shifted to 708 and 723  $\text{cm}^{-1}$  and their lines intensities decreased by 38% and 40%, respectively. It suggested that damage of the C—S bond of trans form was stronger. The double peak of Tyr at 836 and 850  $\text{cm}^{-1}$ , which arose from the Fermi resonance between a ring-breathing vibration and overtone of an out-of plan ring bending vibration<sup>[47–49]</sup>, was changed upon the photosensitive damage. The decrease rates of line intensities at 836 and 850  $\text{cm}^{-1}$  were 9% and 24%, and shifted from 832, 851  $\text{cm}^{-1}$  to 836, 850  $\text{cm}^{-1}$ . The intensity ratio ( $I_{850}/I_{830}$ ) was 0.78, so the Tyr was still “buried”<sup>[47–49]</sup>.

As mentioned above the space structure of viral proteins has been changed clearly, which would directly affect the biological functions of reversed transcriptase, integrase and protease and various capsid proteins in the viral protein. The laser irradiation of HC generates  $^1\text{O}_2$ ,  $\text{O}_2^{\bullet}$ ,  $\bullet\text{OH}$  and  $\text{HC}^{\bullet}$ <sup>[40–44]</sup>, which damage hydrogen bonds that support the space struc-

ture of viral protein molecule. Additionally the organization of the hydrogen bonds might be affected by the HC-induced photosensitive damage of the side-chain of some amino acids located in the  $\alpha$ -helix and  $\beta$ -sheet regions<sup>[49]</sup>. These effects eventually damage  $\alpha$ -helix,  $\beta$ -sheet and  $\beta$ -turn. The photosensitive damage of the main-chain changes the environment of the side-chain, which in turn affects the conformation of the side-chain<sup>[49]</sup>.

(iii) The photosensitive damage of the viral RNA

The backbone phosphate groups: The line assigned phosphate diester ( $\text{PO}_2$ ) symmetric stretching, which is sensitive to RNA conformation change, shifted from 814  $\text{cm}^{-1}$  to 808  $\text{cm}^{-1}$ . This indicated that the A form viral RNA becomes disordered<sup>[3,28]</sup>. The line assigned to backbone phospho ion ( $\text{PO}_2^-$ ) symmetric stretching<sup>[27,28]</sup> shifted from 1106  $\text{cm}^{-1}$  to 1102  $\text{cm}^{-1}$ . The line was found to be relatively insensitive to conformation of RNA<sup>[28]</sup>, then it was usually considered as an internal standard<sup>[28]</sup>. The obvious shift of the line implied that the phosphate ions ( $\text{PO}_2^-$ ) might be the sites of interaction of RNA and hypericin.

The ribose: The line intensities of ribose at 631  $\text{cm}^{-1}$ <sup>[27,28]</sup> decreased by 52%, GlcNac also contributed to the line at 631  $\text{cm}^{-1}$ , whereas that at 974  $\text{cm}^{-1}$ <sup>[27,28]</sup> increased by 206% and shifted to 976  $\text{cm}^{-1}$ . HC is known to generate  $\bullet\text{OH}$  free radical under the irradiated condition<sup>[40]</sup>. If  $\bullet\text{OH}$  free radical abstracts a hydrogen atom from the sugar in C-1 and C-5 positions, the covalent bond between ribose and base as well as the phosphate diester bond would be broken and the ribose would be damaged<sup>[64]</sup>. This would change the ribose and its force bearing environment to make its Raman activity increase so the intensity of the Raman line of the ribose increases.

The bases: The line intensities belonging to various groups of bases had changed. The lines intensities assigned to the cytosine and uracil ring at 786  $\text{cm}^{-1}$ , to the guanine ring at 1322  $\text{cm}^{-1}$ , to the adenine ring at 1341 and 1520  $\text{cm}^{-1}$ , to the guanine and adenine ring at 1419  $\text{cm}^{-1}$ <sup>[27,28]</sup> changed  $-17\%$ ,  $-32\%$ ,  $-35\%$ ,

-54% and -25%, respectively, and their lines shifted to 790, 1320, 1335 and 1514  $\text{cm}^{-1}$ , while the line of C=N, C=C stretching vibration of the guanine and adenine ring at 1579  $\text{cm}^{-1}$  [27,28] almost disappeared. The line intensities at 751(C), 1226(A), 1379(G, U, A), 1484(G, A), 1537  $\text{cm}^{-1}$ (G) [27,28] increased by 47%, 37%, 146%, 20% and 177%, respectively, and their lines shifted to 753, 1231, 1380, 1483 and 1538  $\text{cm}^{-1}$ . The line of the guanine ring at 1365  $\text{cm}^{-1}$  [27,28] changed from shoulder to sharp peak. Two lines of the guanine at 669  $\text{cm}^{-1}$  and cytosine, uracil at 1123  $\text{cm}^{-1}$  [27,28] changed from shoulder peaks to moderate and very strong lines, and their lines shifted to 670 and 1127  $\text{cm}^{-1}$ , respectively. It showed the occurrence of hyperchromic effect, which resulted from disruption of vertical base-base stacking interactions [28,65]. While the carbonyl stretching vibration line of the uracil, guanine and cytosine at 1660  $\text{cm}^{-1}$ , involving interbase hydrogen bonds [28,65], shifted to 1655  $\text{cm}^{-1}$ . This shift was related to the breakage of interbase hydrogen bonds [28,65].

The common line of the groups split into two lines by the HC-induced photosensitive damage at various components of the virus, e.g., the line at 1226  $\text{cm}^{-1}$  split into two lines assigned to  $\beta$ -sheet of the protein at 1228  $\text{cm}^{-1}$  [47-49] and to adenine of the RNA at 1231  $\text{cm}^{-1}$  [27,28]. The line belonging to  $\alpha$ -helix or random coil of the viral protein [47-49] and the uracil, guanine and cytosine, involving interbase hydrogen bonds [28,65], at 1660  $\text{cm}^{-1}$  became two lines assigned to random coil of the viral protein [47-49] at 1664  $\text{cm}^{-1}$  and to the carbonyl stretching vibration of the uracil, guanine and cytosine, involving interbase hydrogen bonds [28,65] at 1655  $\text{cm}^{-1}$ .

As indicated above the backbone phosphate group, ribose and bases of the viral RNA were damaged obviously. Since the viral RNA is an important genetic matter, damages on it would extremely affect the growth and breeding of HIV.

(iv) The photosensitive damage of the viral lipids

The two bands assigned to symmetrical and asymmetrical C—H stretching vibration of methylene

(—CH<sub>2</sub>—) occurred at 2883 and 2848  $\text{cm}^{-1}$  [56,66]. The intensity ratio ( $I_{\text{CH}}$ )  $I_{2883}/I_{2848}$  was about 5.6, and the order parameter for the lateral interaction of lipid— $S_{\text{lat}}$  was about 3.3 [56,66] after photosensitive damage, so viral lipids bilayers still were probably in the liquid ordered phase or gel phase [60,66]. The line assigned to C—N symmetrical stretching vibration of choline group of lipids at 717  $\text{cm}^{-1}$  [58,66] shifted to 723  $\text{cm}^{-1}$  and its intensity decreased by 40%, which was followed by an increase of line width. This suggested that the C—N group was the possible binding site to HC [57,58]. The C—N group is located in hydrophilic head of lipid and has positive changes on it. It might be attacked easily by highly active oxygen species, such as the superoxide anion radical ( $\text{O}_2^{\bullet-}$ ), the hydroxide radical  $\bullet\text{OH}$ , etc. produced by HC photosensitization [40,58].

In summary, hypericin-induced photosensitive damage of HIV1-HIV2 in human serum changed various components of HIV1-HIV2 in different degrees: The orderly A-form viral RNA becomes a disordered viral RNA. There were a breakage of interbase hydrogen bonds and disruption of vertical base-base stacking interactions. In addition, the groups of the ribos and four bases were damaged obviously. A decrease in orderly structure ( $\alpha$ -helix and  $\beta$ -sheet) of viral protein is accompanied by increase in random coil. Damage of the C—S bond of trans form was stronger. The Tyr buried in the three-dimensional structure of protein was also damaged, but it was still "buried". The groups of carbohydrates, including D-Mannos and N-acetyl glucosamine, in viral envelope glycoprotein had been changed. The hydrophilic C—N bond of choline in viral lipid was damaged, which is the possible binding site to hypericin, whereas the viral lipids bilayers were still probably in the liquid ordered phase or the gel phase, so the space structure of HIV1-HIV2 was damaged under the experimental conditions, which might block viral infection and inhibit its growth and breeding. It is apparent that the laser Raman spectra have provided certain direct evidence at the molecular level for photosensitive damage of HIV1-HIV2.

**Acknowledgements** This work was supported by the National Natu-

ral Science Foundation of China (Grant No. 39570189). We thank Profs. Chen Jenweng and Li Gouhua for assistance in the experiment. We also thank Mr. Xia Guang, Dr. G.T.Yu and Dr. Diwu Zhenjun for their revision on English manuscript and their helpful discussion.

## References

1. Thomas, G. J. Jr., Applications of Raman spectroscopy in structural studies of viruses, nucleoproteins and their constituents, in *Spectroscopy of Biological Systems* (eds. Clark, R. J. H., Hester, R. E.), Vol. 13, New York: John Wiley & Sons, 1986, 233–303.
2. Thomas, G. J. Jr., Viruses and Nucleoproteins, in *Biological Applications of Raman Spectroscopy* (ed. Spiro, T. G.), Vol. 1, New York: John Wiley & Sons, 1987, 135–201.
3. Xu, Y. M., Lu, C. Z., Raman spectroscopic study on human immunodeficiency virus (HIV1—HIV2) space structure and microcosmic and photosensitive damage to the virus, *Proceedings of the XVth International Conference on Raman Spectroscopy* (eds. Asher, S. A., Stein, P.), August 11–16, 1996, Pittsburgh, PA, USA, New York: John Wiley & Sons, Ltd., 490–491.
4. Coffin, J., Ashley, H., Jay, A. et al., What to call the AIDS virus? *Nature*, 1986, 321: 10.
5. Weiss, R. A., How does HIV cause AIDS? *Science*, 1993, 260: 1273–1279.
6. Gallo, R. C., Montagnier, L., AIDS in 1988, *Sci. Am.*, 1988, 259: 25–32.
7. Greene, W. C., AIDS and the immune system, *Sci. Am.*, 1993, 269: 67–73.
8. Haseltine, W. A., Wong, S. F., The molecular biology of the AIDS virus, *Sci. Am.*, 1988, 259: 34–42.
9. McDougal, J. S., Kennedy, M. S., Sligh, J. M. et al., Binding of HTLV-III/LAV to T4<sup>+</sup> T cell by a complex of the 110 K viral protein, *Science*, 1986, 31: 382–385.
10. Klatzmann, D., Champagne, E., Chamaret, S. et al., T-lymphocyte T4 molecule behaves as the resepto for human retrovirus, *Nature*, 1984, 312: 767–768.
11. Greene, W. C., The molecular biology of human imunodeficiency virus type 1 infection, *N.E.J. Med.*, 1991, 324: 308–317.
12. Pantaleo, G., Graziosi, C., Demarest, J. F. et al., HIV infection is active and pgressive in lymphoid tissue during the clinically latent stage of disease, *Nature*, 1993, 362: 355–358.
13. Feinberg, M. B., Greene, W. C., Molecular insights into human immunodeficiency virus type-1 pathogenesis, *Curr. Opin. in Immun.*, 1992, 4: 466–474.
14. Cheng Li, in *Medical and Molecular Virology* (ed. Wen Y. M.), Beijing: People's and Medical Press, 1990, 193–202.
15. Wang, X. Z., *Medical Virology Basis, Fundamental Techniques & Methods*, Beijing: Academy Press, China, 1987, 34–44.
16. Feizi, T., Larkin, M., AIDS and glycosylation, *Glycobiology*, 1990, 1: 17–23.
17. Chau, S. N., Ho, D. D., Sun, C. R. Y. et al., Generation and characterization of monoclonal antibodies to the putative CD4-binding domain of human immunodeficiency virus type 1 gp120, *J. Virol.*, 1989, 63: 3579–3585.
18. Richards, A. D., Phylip, L. H., Farmerie, W. G. et al., Sensitive, soluble chromogenic substrates for HIV-1 protease, *J. Biol. Chem.*, 1990, 265: 7733–7736.
19. Cohen, J., Weiee, R. A., Bloom, B. R. et al., The new face of AIDS, *Science*, 1996, 272: 1855–1890.
20. Ho, D. D., Kaplan, J. C., Rackauskas, I. E. et al., Second conserved domain of gp120 is important for HIV infectivity and antibody neutralization, *Science*, 1988, 239: 1021–1023.
21. Rusche, J. R., Javaherian, K., McDanal, C. et al., Antibodies that inhibit fusion of human immunodeficiency virus-ifected cells bind a 24-amino acid sequence of the viral envelope, gp120, *Proc. Natl. Acad. Sci., USA*, 1988, 85: 3198–3202.
22. Kowalski, M., Potz, J., Basiripour, L. et al., Functional regions of the envelope glycoprotein of human immunodeficiency virus type 1, *Science*, 1987, 237: 1351–1355.
23. Gelderblom, H. R., Hausmann, E. H. S., Ozel, M. et al., Fine structure of human immunodeficiency virus (HIV) and immunolocalization of structural proteins, *Virology*, 1987, 156: 171–176.
24. Veronese, F. M., DeVico, A. L., Copeiand, T. D. et al., Characterization of gp41 as the trans- membrane protein coded by the HTLV-III/LAV envelope gene, *Science*, 1985, 229: 1402–1405.
25. Darke, P. L., Leu, C. T., Davis, L. J., Human immunodeficiency virus protease, *J. Biol. Chem.*, 1989, 264: 2307–2312.
26. Larder, R. A., Purifoy, D. J. M., Powell, K L. et al., Structural studies of the acquired immunodeficiency syndrome virus reverse transcriptase, *Am. J. Med.*, 1988, 85: 173–175.
27. Hartman, K. A., Clayton, N., Thomas, G. J. Jr., Studies of virus structure by Raman spectroscopy I. R17 virus and R17 RNA, *Biochem. Biophys. Res. Commun.*, 1973, 50: 942–949.
28. Thomas, G. J. Jr., Prescott, B., Studies of virus structure by laser-Raman spectroscopy (II): MS2 phage, MS2 capsids and MS2 RNA in aqueous solutions, *J. Mol. Biol.*, 1976, 102: 103–124.
29. Frankel, A. D., Young, J. A. T., HIV-1: Fifteen Proteins and an RNA, *Annu. Rev. Biochem.*, 1998, 67: 1–25.
30. Marx, J. L., AIDS drugs – coming but not have, *Science*, 1989, 244: 287.
31. Holden, C., Treating AIDS with worts, *Science*, 1991, 25: 522.
32. Schinazi, R. F., Chu, C. K., Babu, J. R. et al., Antraquionones as a class of antiviral agents against human immunodeficiency virus, *Antiviral Res.*, 1990, 13: 265–272.
33. Takahashi, I., Nakanishi, S., Kobayashi, E. et al., Hypericin and pseudohypericin specifically inhibit protein kinase C: Possible relation to their anti-retroviral activity, *Biochem. Biophys. Res. Commun.*, 1989, 165: 1207–1212.
34. Diwu, Z., Zimmermaun, J., Meyer, T. et al., Design, synthesis and investigation of mechanisms of action of novel protein kinase C inhibitors: Perylenequinonoid pigments, *Biochem. Pharmacol.*, 1994, 47: 373–385.
35. Lenard, J., Rabson, A., Stevenson, N. R. et al., Photodynamic inactivation of viral fusion and infectivity by hypericin and rose bengal: Effects on HIV and other enveloped virus, *J. Cell. Biochem.*, 1993, 17 E–F, 17.
36. Lenard, J., Rabson, A., Vanderoef, R., photodynamic inactivation of infectivity of human immunodeficiency virus and other enveloped virus using hypericin and rose Bengal: Inhibition of fusion and syncytia formation, *Proc. Natl. Sci. USA*, 1993, 90: 158–162.

37. Fields, A. P., Bednarik, D. P., Hess, A. et al., Human immunodeficiency virus induces phosphorylation of its cell surface receptor, *Nature*, 1988, 333: 278–280.
38. Degar, S., Prince, A. M., Pascual, D. et al., Inactivation of the human immunodeficiency virus by hypericin: evidence for photochemical alterations of p24 and ablock in uncoating, *AIDS Res. Hum. Retroviruses*, 1992, 8: 1929–1936.
39. Meruelo, D., Lavie, G., Lavie, D., Therapeutic agents with dramatic antiretroviral activity and little toxicity at effective doses: Aromatic polycyclic diones hypericin and pseudohypericin, *Proc. Natl. Acad. Sci. USA*, 1988 85: 5230–5234.
40. Diwu Zhenjun, Novel therapeutic and diagnostic applications of hypocrellins and hypericins, *Photochem. and Photobiol.*, 1995, 61: 529–539.
41. Lopez-Bazzocchi, I., Hudson, J. B., Towers, G. H. N., Antiviral activity of the photoactive plant pigment hypericin, *Photochem. and Photobiol.*, 1991, 54: 95–98.
42. Hudson, J. B., Imperial, V., Haugland, R.P., Diwu, Z., Antiviral activities of photoactive perylenequinones, *Photochemistry and Photobiology*, 1997, 65: 352–354.
43. Hudson, J. B., Harris, L., Towers, G. H. N., The importance of light in the anti-HIV effect of hypericin, *Antiviral Res.*, 1993, 20: 173–178.
44. Meruelo, D., Prince, A. M., Pascual, D. et al., The potential use of hypericin as inactivator of retroviruses and other viruses in blood products, *Blood*, 1993, 82: 205A.
45. Dougherty, T. J., Photodynamic therapy, *Photochemistry and Photobiology*, 1993, 58: 895–900.
46. Lavie, G. F., Valentine, G., Levin, Y. et al., Studies of the mechanisms on action of the antiretroviral agent hypericin and pseudohypericin, *Proc. Natl. Acad. Sci. USA*, 1989, 86: 5963–5967.
47. Lord, R. C., Yu, N. T., Laser-Raman spectroscopy of biomolecules (I): Native lysozyme and its constituent amino acids, *J. Mol. Biol.*, 1970, 50: 509–524.
48. Carey, P. R., *Biochemical Applications of Raman and Resonance Raman Spectroscopies*, New York: Harcourt Brace Jovanovich, 1982, 71–98.
49. Zhang, Z. Y., Xu, Y. M., The Molecular of photoporphyrin (YHPD)'s photosensitization, *Science in China, Ser. B*, 1992, 35: 437–444.
50. Koenig, J. L., *Infrared and Raman Spectroscopy of Biological Molecules* (ed. Theophanides, M. T.), Holland: NATO Scientific Affairs Division, 1979, 109–125, 125–137.
51. Parker, F. S., *Applications of Infrared, Raman, and Resonance Raman Spectroscopy in Biochemistry*, New York: Plenum Press, 1983, 315–347.
52. Zhao, H., Xu, Y. M., Lu, C. Z., Raman spectroscopic study of D-Mannose after the photosensitive damage caused by hypericin, *Int. Asian J. of Spectroscopy*, 1997, 1: 71–76.
53. Krimm, S., Bandekar, J., Vibrational analysis of peptides, polypeptides, and proteins, Normal vibrations of  $\beta$ -turn, *Biopolymers*, 1980, 19: 1–29.
54. Bandekar, J., Krimm, S., Vibrational analysis of peptides, polypeptides, and proteins (VI): Assignment of  $\beta$ -turn modes in insulin and other proteins, *Biopolymers*, 1980, 19: 31–36.
55. Thomas, G. J. Jr., Kyogoku Yoshimasa, Biological Science, in *Infrared and Raman Spectroscopy, Part C* (eds. Bram, E. G. Jr. et al.), New York and Basel: Marcel Dekker, Inc., 1977, 778–782.
56. Tu, A. T., *Raman Spectroscopy in Biology: Principles and Applications*, New York: John Wiley and Sons, Inc., 1982, 187–205.
57. Xu, Y. M., Zhao, H. X., Zhang, Z. Y., Raman spectroscopic study of microcosmic and photosensitive damage on the liposomes of the mixed phospholipids sensitized by hypocrellin and its derivatives, *Int. J. Photochem. & Photobiol. B: Biol.*, 1998, 43: 41–46.
58. Xu, Y. M., Zhang, Z. Y., Zhang, W., Raman spectroscopic characteristics of microcosmic and photosensitive damage on space structure of liposomes sensitized by hypocrellin and its derivatives, *Science in China, Ser. C*, 1998, 41(5): 460–464.
59. Xu, Y. M., Yang, H. Y., Zhing, Z. Y., Raman spectroscopic study of space structure of membrane proteins and membrane lipids in photodamaged human erythrocyte sensitized by hypocrellin B, *Science in China, Ser. C*, 1998, 41(7): 608–616.
60. Brown, D. A., London, E., Structure and origin of ordered lipid domains on biological membranes, *J. Membrane Biol.*, 1998, 164: 103–114.
61. Brunner, H., Sussner, H., Raman scattering of native and thermally denatured lysozyme, *Biochim. Biophys. Acta*, 1972, 271: 16–22.
62. Xu, Y. M., Zhang, Z. Y., Zhao, K. J. et al., Molecular mechanism of high energy proton radiation—Raman spectroscopic character of microcosmic damage in the space structure of DNA, *Science in China, Ser. B*, 1993, 36: 1325–1332.
63. She, C. Y., Dinh, N. D., Tu, A. T., Laser Raman scattering of glucosamine, N-acetylglucosamine and glucuronic acid, *Biochim. Biophys. Acta*, 1974, 372: 345–355.
64. Kuwabara, M., Zhang, Z. Y., Yosaii, G., E.S.R. of spin trapped radicals in aqueous solutions of Pyrimidine nucleosides and nucleotides, Reaction of the Hydroxyl Radicals *Int. J. Radiat. Biol.*, 1982, 41: 241–259.
65. Erfurth, S. C., Peticolas, W. L., Melting and premelting phenomenon in DNA by Laser Raman scattering, *Biopolymer*, 1975, 14: 247–264.
66. Gaber, B. P., Peticolas, W. L., On the quantitative interpretation of biomembrane structure by Raman spectroscopy, *Biochim. Biophys. Acta*, 1977, 465: 260–274.